

Experimental and theoretical analysis of antibacterial molecule N,N,N,N-Cetyltrimethylammonium bromide

G.Bagavathi Sankar¹, D.Usha²

¹Reg.No18223282131003, Department of Physics, St.Johns College of Arts and Science Ammandivilai

²Associate Professor, Department of Physics, Womens Christian College, Nagercoil-629001

^{1,2}Affiliated to Manonmaniam Sundaranar University, Abishekapatti, Tirunelveli-627 012, Tamilnadu, India

Abstract

N,N,N,N-Cetyltrimethylammonium bromide (NCT) has been investigated using DFT/B3LYP/6-311++G(d,p) basis set which is supported by FMO and MEP analysis. From these studies, Molecular interactions, charge delocalization and electrophilic and nucleophilic sites within the reactant types have been also explored. Assisted by DFT optimizations executing a tight convergence norm, vibrational frequencies and topology analysis were carried.

1. Introduction

Cetyltrimethylammonium bromide (CAB) is a quadrivalent ammonium surface-active agent and also it is the constituents of the interesting antibacterial cetrimide [1]. The cetrimonium (hexadecyltrimethylammonium) cation is an active germ-killing agent used in contrast to bacteria and fungi. In addition, it is also the main constituents of some barriers for the removal of DNA [2]. It has been extensively used in production of gold nanoparticles too hair conditioning yields. Cetrimonium chloride and cetrimonium stearate are used as contemporary antiseptics and found in many domestic goods shampoos and cosmetics. CAB has developed for biological expenditure as it keeps the precipitated DNA in its isolation [3]. Cells characteristically obligate high applications of macromolecules glycoproteins and polysaccharides which in the extraction process co-precipitate with DNA, causing the extracted DNA to lose purity. The positive charge of the CAB molecule allows it to denature these molecules that would interfere with this isolation [2]. CAB has been revealed to have potential use as an apoptosis-promoting anticancer agent for head and neck cancer [4]. CAB revealed anticancer cytotoxicity against several HNC cell lines with minimal effects on normal fibroblasts, a selectivity that exploits cancer-specific metabolic aberrations. CAB is also suggested by the World Health Organisation as a purification agent in the downstream vaccine processing of polysaccharide vaccines. Cetrimonium bromide (Cetyltrimethylammonium bromide or CTAB) is a surfactant and antiseptic agent with various antibacterial, antifungal and antiviral properties. N,N,N,N-Cetyltrimethylammonium bromide (NCT) is an antibacterial active molecule. By reason of the extensive range of applications of NCT received a great interest in chemical biology and pharmaceutical chemistry

research fields. Therefore, its derivatives show a broad variety of bioactivities; hereafter, studies of their molecular structure have great importance for rational drug designs and other uses. To explore the detailed molecular structure and the vibrational spectral modes of NCT with bioactive molecule this shows significant antimicrobial activities against bacterial pathogens. It is very vital to study the spectroscopic and structural properties of a molecule to understand its chemical and biological behavior. The calculated FT-IR and FT-Raman spectra were compared with the experimental results.

2. Experimental Details

FTIR spectrum recorded using Perkin Elmer Spectrometer using KBr pellet method. FT Raman spectrum was recorded using BRUKER RFS 27: Stand alone FT Raman Spectrometer and the laser source were used Nd: YAG 1064 nm with spectral resolution of 2.0 cm⁻¹. UV-VIS absorption spectrum in methanol as a solvent is scrutinized in the range 200-800 nm with spectral Bandwidth 2nm using UV-VIS spectrophotometer. The antimicrobial activity of DAP was screened by agar well diffusion method.

3. Computational Details

Quantum chemical computational method has been implemented using B3PW91/6-31++G(d,p) basis set by the Gaussian '09 program [5]. UV-vis spectra, electronic transitions, excitation energies, absorbance and oscillator strengths were calculated with the time-dependent DFT method [6-9]. Natural bond orbital (NBO) analysis was executed using NBO 3.1 program [10]. The illustrative suggestion of the intermolecular interactions collected from the ELF, LOL, RDG properties were achieved using multiwfn multifunctional wave function analyzer [11,12] and plotted with VMD molecular visualisation program [13].

4. Results and Discussion

4.1 Structural Analysis

The optimized parameters of NCT with atoms numbering is given in Fig. 1 and the optimized geometrical parameter such as bond lengths, bond angles, and dihedral angles of NCT are attained in the B3LYP/6-311 ++ G (d,p) basis set, and their values are given in Table 1.

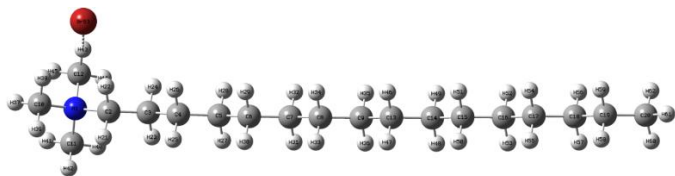


Fig 8.1 Optimized structure of NCT

Global minimum energy of NCT is -3375.90 Hartrees. N1-C2 and N1-C10 bond lengths of NCT are 1.5 Å while N1-C11 bond length is 1.4 Å which suggests that N1-C11 bond length is not affected by the intermolecular hydrogen bonding interaction. Methyl group electron donor and acceptor

capabilities accept a major contract in molding the elements' structure and electronic properties. The methyl group shares its lone pair electrons with the π electrons in a side chain, methylene group and the methyl group interacts with the nearby π systems. The methyl, methylene, and bromine atom of the NCT may perhaps suggest inter and intra-molecular interactions. Intermolecular contacts of H22...Br63, H38...Br63 and H43...Br63 are 2.4653, 2.5429 and 2.51 Å respectively which are considerably smaller than the van der Waals separations showing the opportunity of the intermolecular C-H...Br hydrogen bonding in NCT. This is proved that the most potent antibacterial activity exhibited by the compound is due to the presence of intermolecular C-H...Br hydrogen bonding.

Table 1 Optimized Parameters of NCT

Bond length	NCT (Å)	Bond Angle	NCT (°)	Dihedral Angle	NCT (°)
N1-C2	1.5365	C2-N1-C10	107.0905	C10-N1-C2-C3	174.4776
N1-C10	1.513	C2-N1-C11	111.1944	C10-N1-C2-H21	62.3877
N1-C11	1.496	C2-N1-C12	110.8743	C10-N1-C2-H22	53.0163
N1-C12	1.5124	C10-N1-C11	109.4781	C11-N1-C2-C3	65.9594
C2-C3	1.5244	C10-N1-C12	108.1504	C11-N1-C2-H21	57.1753
C2-H21	1.0949	C11-N1-C12	109.9556	C11-N1-C2-H22	172.5793
C2-H22	1.0988	N1-C2-C3	116.1855	C12-N1-C2-C3	56.6996
C3-C4	1.5396	N1-C2-H21	105.0935	C12-N1-C2-H21	179.8343
C3-H23	1.0984	N1-C2-H22	104.329	C12-N1-C2-H22	64.7617
C3-H24	1.0954	C3-C2-H21	111.0193	C2-N1-C10-H37	179.2506
C4-C5	1.5339	C3-C2-H22	110.1559	C2-N1-C10-H38	60.4882
C4-H25	1.0994	H21-C2-H22	109.6862	C2-N1-C10-H39	59.6064
C4-H26	1.097	C2-C3-C4	109.3655	C11-N1-C10-H37	58.5907
C5-C6	1.5345	C2-C3-H23	112.1633	C11-N1-C10-H38	178.8518
C5-H27	1.1002	C2-C3-H24	110.164	C11-N1-C10-H39	61.0535
C5-H28	1.0992	C4-C3-H23	109.2681	C12-N1-C10-H37	61.2052
C6-C7	1.5343	C4-C3-H24	108.1883	C12-N1-C10-H38	59.0559
C6-H29	1.099	H25-C3-H24	107.5975	C12-N1-C10-H39	179.1505
C6-H30	1.0998	C3-C4-C5	112.9149	C2-N1-C11-H40	62.3581
C7-C8	1.5344	C3-C4-H25	109.5931	C2-N1-C11-H41	177.7503
C7-H31	1.1001	C3-C4-H26	108.4729	C2-N1-C11-H42	57.9655
C7-H32	1.0997	C5-C4-H25	109.3202	C10-N1-C11-H40	179.5112
C8-C9	1.5344	C5-C4-H26	109.6567	C10-N1-C11-H41	59.6196
C8-H33	1.0998	H25-C4-H26	106.6898	C10-N1-C11-H42	60.1652
C8-H34	1.0995	C4-C5-C6	113.2119	C12-N1-C11-H40	60.829
C9-H13	1.5345	C4-C5-H27	109.5441	C12-N1-C11-H41	59.0626
C9-H35	1.0998	C4-C5-H28	109.1042	C12-N1-C11-H42	178.8474
C9-H36	1.1	C6-C5-H27	109.3152	C2-N1-C12-H43	53.4273
C10-H37	1.0916	C6-C5-H28	109.1267	C2-N1-C12-H44	67.8264
C10-H38	1.0983	H27-C5-H28	106.3044	C2-N1-C12-H45	172.8382
C10-H39	1.0915	C5-C6-C7	113.4456	C10-N1-C12-H43	63.7028

C11-H40	1.0895	C5-C6-H29	109.0884	C10-N1-C12-H44	175.0436
C11-H41	1.0914	C5-C6-H30	109.3158	C10-N1-C12-H45	55.7082
C11-H42	1.0915	C7-C6-H29	109.3367	C11-N1-C12-H43	176.8019
C12-H43	1.0988	C7-C6-H30	109.2854	C11-N1-C12-H44	55.5482
C12-H44	1.0895	29-C6-H30	106.1074	C11-N1-C12-H45	63.7871
C12-H45	1.0915	C6-C7-HC8	113.5853	N1-C2-C3-C4	178.3883
C13-C14	1.5345	C6-C7-H31	109.3093	N1-C2-C3-H23	60.2218
C13-H46	1.0997	C6-C7-H32	109.1506	N1-C2-C3-H24	59.6028
C13-H47	1.0998	C8-C7-H31	109.2671	H21-C2-C3-C4	61.624
C14-C15	1.5345	C8-C7-H32	109.152	H21-C2-C3-H23	59.7659
C14-H48	1.0999	H31-C7-H32	106.1058	H21-C2-C3-H24	179.5905
C14-H49	1.0998	C7-C8-C9	113.5907	H22-C2-C3-C4	60.0755
C15-C16	1.5345	C7-C8-H33	109.3014	H22-C2-C3-H23	178.5346
C15-H50	1.0998	C7-C8-H34	109.12	H22-C2-C3-H24	58.7099
C15-H51	1.0998	C9-C8-H33	109.2559	N1-C2-H22-Br63	24.2759
C16-H17	1.5345	C9-C8-H34	109.2256	C3-C2-H22-B63	101.0986
C16-H52	1.0998	H33-C8-H34	106.0738	H21-C2-H22-63	136.4133
C16-H53	1.0999	C8-C9-C13	113.6537	C2-C3-C4-C5	179.7855
C17-H18	1.5344	C8-C9-H35	109.172	C2-C3-C4-H25	57.6626
C17-H54	1.0998	C8-C9-H36	109.2583	C2-C3-C4-H26	58.4613
C17-H55	1.0998	C13-C9-H35	109.1608	H23-C3-C4-C5	56.6605
C18-C19	1.5345	C13-C9-H36	109.2522	H23-C3-C4-H25	65.4624
C18-H56	1.1	H35-C9-H36	106.0657	H23-C3-C4-H26	178.4137
C18-H57	1.1	C1-C10-H37	108.4187	H24-C3-C4-C5	60.2094
C19-C20	1.5331	C1-C10-H38	107.2559	H24-C3-C4-H25	177.6677
C19-H58	1.0989	C1-C10-H39	108.4094	H24-C3-C4-H26	61.5439
C19-H59	1.0989	H37-C10-H38	111.2772	C3-C4-C5-C6	178.8237
C20-H60	1.0966	H37-C10-H39	110.211	C3-C4-C5-H27	58.8911
C20-H61	1.0955	H38-C10-H39	111.1416	C3-C4-C5-H28	57.0993
C20-H62	1.0966	N1-C11-H40	109.5767	H25-C4-C5-C6	58.9003
H22- Br 63	2.4653	N1-C11-H41	108.8344	H25-C4-C5-H27	63.3849
H38- Br 63	2.5429	N1-C11-H42	108.9634	H25-C4-C5-H28	179.3753
H43-Br63	2.51	H40-C11-H41	109.6479	H26-C4-C5-C6	57.7402
		H40-C11-H42	109.9374	H26-C4-C5-H27	179.9746
		H41-C11-H42	109.8598	H26-C4-C5-H28	63.9842
		N1-C12-H43	107.2812	C4-C5-C6-C7	179.0561
		N1-C12-H44	109.0257	C4-C5-C6-H29	56.9158
		N1-C12-H45	107.8705	C4-C5-C6-H30	58.7033
		H43-C12-H44	111.8084	H27-C5-C6-C7	58.5312
		H43-C12-H45	110.8009	H27-C5-C6-H29	179.3285
		H44-C12-H45	109.9241	H27-C5-C6-H30	63.7094
		C9-C13-C14	113.6106	H28-C5-C6-C7	57.3444
		C9-C13-H46	109.1564	H28-C5-C6-H29	64.7959

		C9-C13-H47	109.2829	H28-C5-C6-H30	179.585
		C14-C13-H46	109.2139	C5-C6-C7-C8	179.0395
		C14-C13-H47	109.2442	C5-C6-C7-H31	58.652
		H46-C13-H47	106.0569	C5-C6-C7-H32	56.9961
		C13-C14-C15	113.6824	H29-C6-C7-C8	57.0373
		C13-C14-H48	109.2448	H29-C6-C7-H31	179.3458
		C13-C14-H49	109.1734	H29-C6-C7-H32	65.0062
		C15-C14-H48	109.2407	H30-C6-C7-C8	58.703
		C15-C14-H49	109.1653	H30-C6-C7-H31	63.6055
		C48-C14-H49	106.0532	H30-C6-C7-H32	179.2536
		C14-C15-H16	113.621	C6-C7-C8-C9	179.908
		C14-C15-H50	109.2713	C6-C7-C8-H33	57.8
		C14-C15-H51	109.1739	C6-C7-C8-H34	57.7885
		C16-C15-H50	109.2378	H31-C7-C8-C9	57.7601
		C16-C15-H51	109.2074	H31-C7-C8-H33	64.5319
		H50-C15-H51	106.0524	H31-C7-C8-H34	179.8796
		C15-C16-C17	113.6914	H32-C7-C8-C9	57.8654
		C15-C16-H52	109.1837	H32- C7-C8-H33	179.8427
		C15-C16-H53	109.2344	H32- C7-C8-H34	64.2542
		C17-C16-H52	109.1777	C7-C8-C9 -C13	179.0697
		C17-C16-H53	109.2228	C7-C8-C9 -H35	56.9524
		H52-C16-H53	106.0489	C7-C8-C9 -H36	58.6314
		C16-C17-C18	113.6447	H33-C8-C9-C13	58.6132
		C16-C17-H54	109.1877	H33- C8-C9-H35	179.2695
		C16-C17-H55	109.254	H33- C8-C9-H36	63.6857
		C18-C17-H54	109.2037	H34- C8-C9-C13	57.0087
		C18-C17-H55	109.2201	H34- C8-C9-H35	65.1086
		H54-C17-H55	106.0521	H34- C8-C9-H36	179.3076
		C17-C18-C19	113.7226	C8-C9-C13-C14	179.9474
		C17-C18-H56	109.2417	C8-C9-C13-H46	57.8027
		C17-C18-H57	109.2709	C8-C9-C13-H47	57.7756
		C19-C18-H56	109.1296	H35- C9-C13-C14	57.8239
		C19-C18-H57	109.1569	H35- C9-C13-H46	64.3209
		H56-C18-H57	106.034	H35- C9-C13-H47	179.8991
		C18-C19-C20	113.3233	H36- C9-C13-C14	57.7503
		C18-C19-H58	109.196	H36- C9-C13-H46	179.8951
		C18-C19-H59	109.1511	H36- C9-C13-H47	64.5266
		C20-C19-H58	109.4254	N1-C10-H38-Br63	2.6851
		C20-C19-H59	109.4172	H37-C10-H38-Br63	121.1106
		H58-C19-H59	106.0712	H39-C10-H38-Br63	115.6528
		C19-C20-H60	111.1729	N1-C12-H43-Br63	8.3792
		C19-C20-H61	111.4714	H44-C12-43- Br Br	127.865
		C19-C20-H62	111.1503	H45-C12-43- Br 63	109.1347

		H60-C20-H61	107.6671	C9-C13-C14-C15	179.2296
		H60-C20-H62	107.5163	C9-C13-C14-H48	58.4765
		H61-C20-H62	107.6745	C9-C13-C14-H49	57.0858
		C2-22- Br 63	152.5603	H46-C13-C14-C15	57.1168
		C10-H38- Br 63	148.7717	H46-C13-C14-H48	179.4106
		C12-H43- Br 63	149.6863	H46-C13-C14-H49	65.0271
		H22- Br 63-38	53.3238	H47-C13-C14-C15	58.472
		H22- Br 63-H43	57.6653	H47-C13-C14-H48	63.8219
		H38- Br 63-H43	56.4549	H47-C13-C14-H49	179.3842
				C13-C14-C15-C16	179.8529
				C13-C14-C15-H50	57.8797
				C13-C14-C15-H51	57.6965
				H48- C14-C15-C16	57.851
				H48- C14-C15-H50	64.4164
				H48- C14-C15-H51	179.9926
				H49- C14-C15-C16	57.7046
				H49- C14-C15-H50	179.972
				H49- C14-C15-H51	64.4518
				C14-C15-C16-C17	179.4719
				C14-C15-C16-H52	57.2982
				C14-C15-C16-H53	58.2589
				H50- C15-C16-C17	58.2422
				H50- C15-C16-H52	179.5841
				H50- C15-C16-H53	64.0271
				H51- C15-C16-C17	57.3341
				H51- C15-C16-H52	64.8396
				H51- C15-C16-H53	179.6033
				C15- C16-C17-C18	179.9274
				C15- C16-C17-H54	57.7493
				C15- C16-C17-H55	57.8246
				H52- C16-C17-C18	57.7504
				H52- C16-C17-54	64.4277
				H52- C16-C17-H54	179.9984
				H52- C16-C17-H55	57.7969
				H53- C16-C17-C18	179.975
				H53- C16-C17-H54	64.4511
				H53- C16-C17-H55	179.6531
				C16-C17-C18-C19	57.4773
				C16-C17-C18-H56	58.1143
				C16-C17-C18-H57	57.484
				H54- C17-C18-C19	64.6919
				H54- C17-C18-H56	179.7166
				H54- C17-C18-H57	58.0801

				H55- C17-C18-C19	179.7441
				H55- C17-C18-H56	64.1525
				H55- C17-C18-H57	179.9269
				C17- C18-C19-C20	57.8237
				C17- C18-C19-H58	57.7208
				C17- C18-C19-H59	57.6892
				H56- C18-C19-C20	179.9385
				H56- C18-C19-H58	64.517
				H56- C18-C19-H59	57.7775
				H57- C18-C19-C20	64.4718
				H57- C18-C19-H58	179.9837
				H57- C18-C19-H59	59.9946
				C18-C19-C20-H60	179.8678
				C18-C19-C20-H61	59.7363
				C18-C19-C20-H62	62.127
				H58- C19-C20-H60	58.0106
				H58- C19-C20-H61	178.1421
				H58- C19-C20-H62	177.9474
				H59- C19-C20-H60	57.8099
				H59- C19-C20-H61	62.3216
				H59- C19-C20-H62	57.0541
				C2-22- Br 63-H38	12.8244
				C2-22- Br 63-H43	35.9346
				C10-38- Br 63-H22	36.2237
				C10-38- Br 63-H43	36.047
				C12-43- Br 63-H22	28.583
				C12-43- Br 63-H38	174.4776

4.2 Vibrational Spectral Analysis

FT IR and Raman spectra as shown in Fig 2 and the vibrational spectral analysis of NCT explained details as given below:

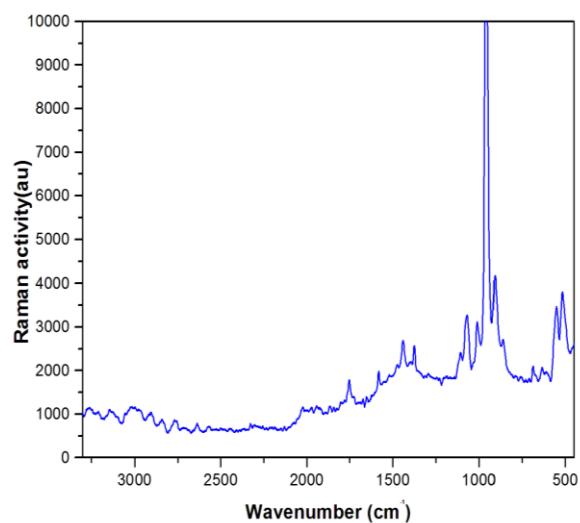
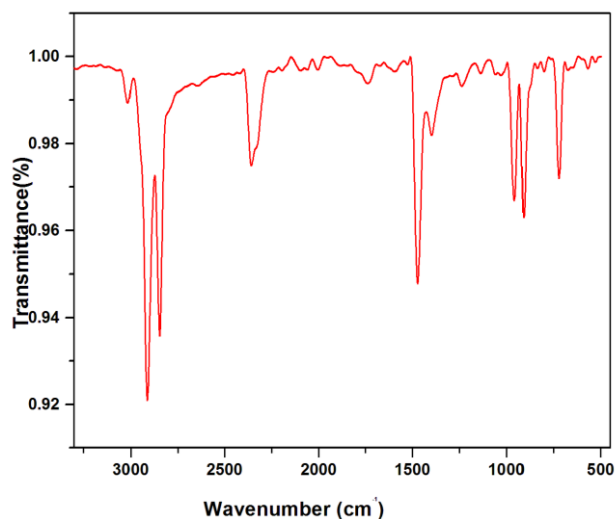


Fig 2 FT IR and FT Raman spectrum of NCT

Table 2 UV-vis wavelength and their contributions of NTE

Energy (cm ⁻¹)	Experimental		Theoretical		Osc. Strength	Symmetry	Major contributions
	Wavelength (nm)	Band gap	Wavelength (nm)	Band gap			
373 59.8 5	200	6.2	207		0.000	Singlet-A	HOMO → LUMO (99%)
373 86.4 7	200	6.2	207		0.001	Singlet-A	HOMO-1 → LUMO (99%),
383 84.9 9			260		0.043	Singlet-A	HOMO-2 → LUMO (99%)

4.2.1 Trimethyl ammonium vibration

Vital vibrational modes of NCT are N-(CH₃)₃, CH₃ stretching and methyl deformation. N-(CH₃)₃ stretching mode can be used as a good probe for assessing the bonding configuration about the ammonium N atom and the electronic distribution of the amine compounds. n → π* conjugation among the ammonium lone pair nitrogen electrons with methyl group system 1374 cm⁻¹ [14, 15]. Methyl groups are generally referred to as electron donating. N-(CH₃)₃ stretching is observed as a medium band at 1374 cm⁻¹ in Raman. Usually CH₃ asymmetric and symmetric stretching vibrations are found around at 2962 and 2872 cm⁻¹ [16, 17]. The asymmetric CH₃ stretching modes at 3015, 2912 cm⁻¹ in IR and at 3014 cm⁻¹ in Raman. Symmetric stretching is observed at 2912, and 2847 cm⁻¹ in IR counterpart with at 2876 2842 cm⁻¹ in Raman. CH₃ stretching mode intensity changes due to the effect of hyperconjugation of methyl group's electronic properties which clearly indicates that methyl hydrogen is directly involved in the donation of electronic charge. Asymmetric and symmetric bending vibrations of methyl group typically seen nearby 1450 and 1375 cm⁻¹ respectively [18]. Asymmetric bending mode of CH₃ group is observed at 1472 in IR and symmetric bending mode of CH₃ group is observed in IR at 1399 cm⁻¹ and in Raman at 1374 cm⁻¹. CH₃ rocking mode of methyl performing as assorted vibrations is expected to take place in the region 1070-900 cm⁻¹ [19, 20] which are observed as strong bands in IR at 1137 counterpart with in Raman at 1068 cm⁻¹ and the strong intensity in IR and Raman wavenumbers of the rocking mode suggests the presence of hyperconjugation.

4.2.2 Methylene Group Vibrations

Asymmetric and symmetric stretching CH₂ vibrations are generally arisen in the region 3000 ± 45 cm⁻¹ and 2950 ± 45 cm⁻¹ respectively [21, 22]. In NCT, this mode is observed at 2912, 2847 cm⁻¹ in IR and 2842 cm⁻¹ in Raman and this is coupled with symmetric stretching.

4.3 Electronic Properties

4.3.1 UV spectral Analysis

The electronic absorption spectrum of NCT compound was computed by TD-DFT with B3LYP/6-311++G(d, p) level. Experimental UV-Vis spectrum is shown in Fig. 3. The oscillator strengths, excitation energies and wavelengths were estimated by using this method and basis set which are given in Table 2. The observed spectrum demonstrated the maximum absorption peaks at 200 nm which indicated that π → π* and n → π* transitions, respectively. According to the theoretical calculations, the bands at 207 and 260 nm were attributed to these transitions. These transitions of oscillator strengths and excitation energies were obtained from simulation results and these data are given in Table 2.

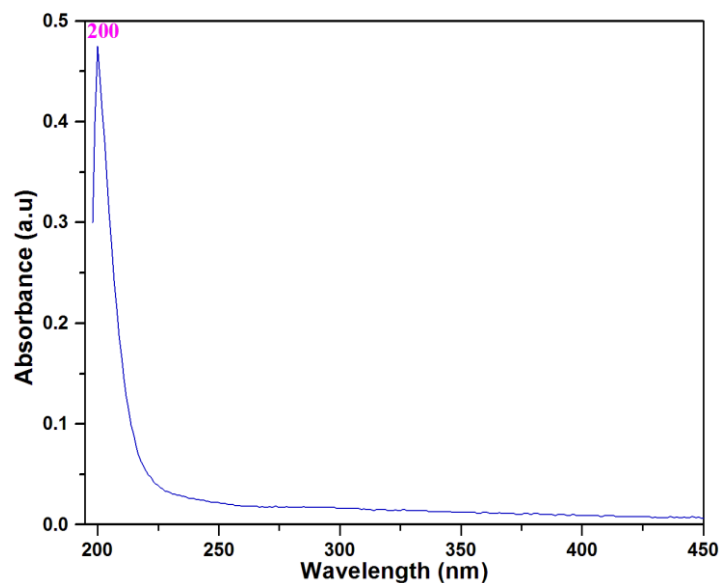


Fig 3 UV Spectra of NCT

4.3.2 FMO analysis

The FMO plots are given in Fig 4. A reaction appliance is a categorization of multi electron transfer steps between donors and acceptors species which is presented as nucleophiles and electrophiles, respectively. The electron transfer depends on the energy gap between HOMO and LUMO within a reactant molecule, the energy difference between the HOMO of the donor and the LUMO of the acceptor. The energies of HOMO, LUMO and HOMO LUMO energy gap are -8.0502, -1.6966 and 6.3535 eV. It is well-known that more polarizable the molecule, the higher its tendency to participate in a chemical change. In fact, small energy gap results in a soft mixing between HOMO and LUMO wave functions which

enhances the bioactivity. The FMO energy gap can be seen in DOS plot as shown in Fig 5.

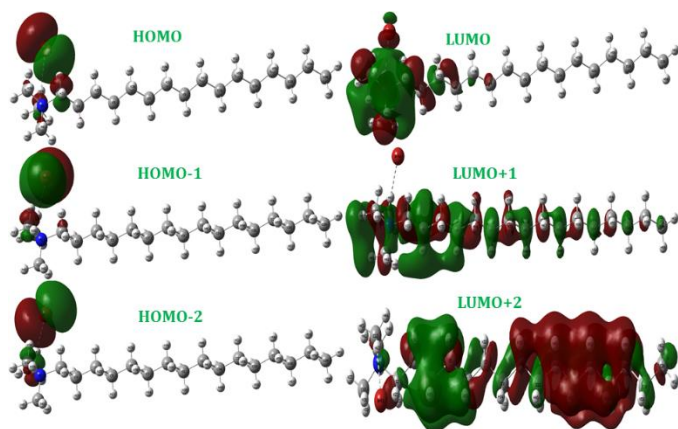


Fig 4 FMO plots

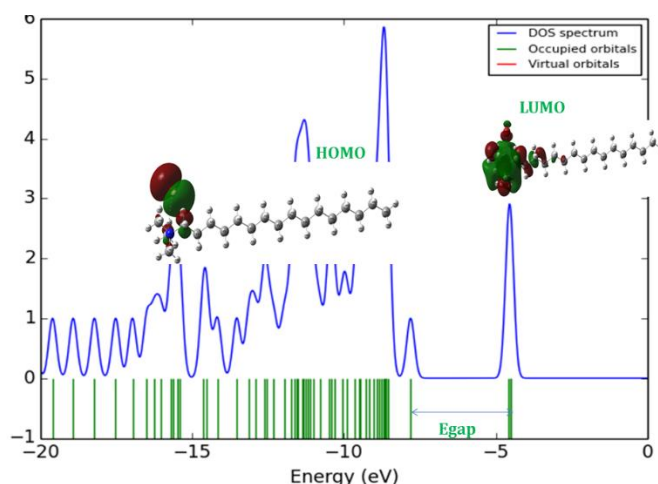


Fig 5 DOS plot of NCT

4.4 Charge Analysis

4.4.1 Electrostatic Potential

Molecular electrostatic potential (MEP) is an important tool for the analysis of molecular interactions, as it aids in locating the reactive site (region) in a molecule and hence determines of an electrophile or nucleophile attack is explained in Fig 6. In MEP, electron-rich region related with electrophilic reactivity is existing by red color although an electron-poor region interrelated to nucleophilic reactivity is given in blue color and in-between colors represent in-between values decreases in the order red > orange > yellow > green > blue.. Though, methyl group carbons have higher potential sites than other methylene groups, therefore trimethyl ammonium has more electrophilic aptitude than other carbons. The presence of trimethylammonium group as a donor and acceptor (Bromine atom) discusses it as a fascinating potential biological and pharmacological properties and, therefore, are of interest as possible drug candidate, as proposed by Veber and Lipinski [23, 24]. From Fig. 6, the strong red colour can be seen on the Br atom that belongs to C-H in methyl group. Blue colours are shown on the H atoms of trimethyl revealing that these sites are clearly electrophilic regions. Note that the large aliphatic side chains are inert regions which present in green colours.

Copyrights @Kalahari Journals

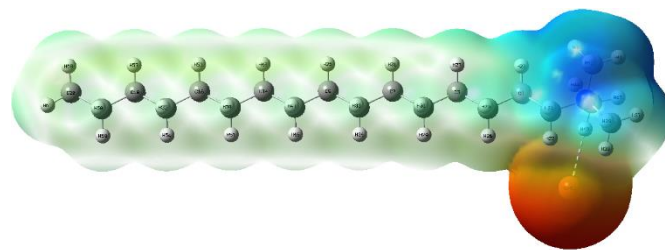


Fig 6 ESP surface of NCT

4.4.2 Natural Charge Analysis

The natural atomic charges plots of NCT are shown in Table 3. It plays an important role in the application of quantum chemical calculation to molecular system because of atomic charges effect dipole moment, molecular polarizability, electronic structure and other molecular properties of molecular systems. The natural charge analysis of NCT shows bromine atom possesses negative charge. The maximum positive atomic charge is obtained for C38 atom when compared with all other atoms is due to the attachment of negatively charged nitrogen atom and the effect of intermolecular hydrogen bonding interaction with bromine atom.

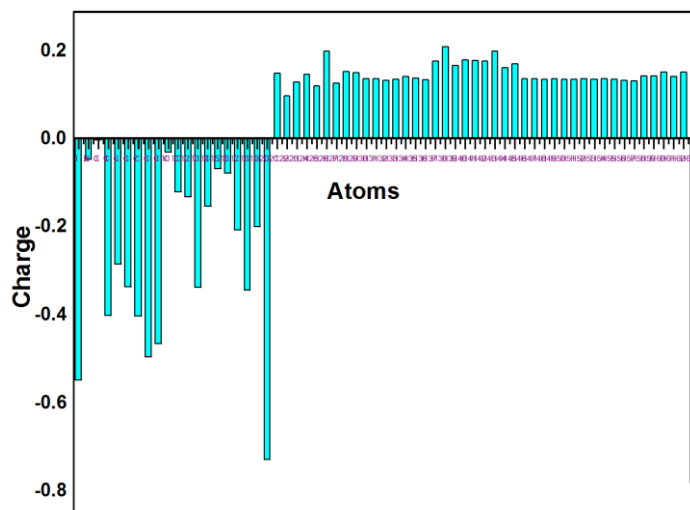


Fig 7 Charge plot of NCT

4.5 Topological Analysis

The topological analyses of the electron localization function (ELF) and the localized orbital locator (LOL) were completed using Multiwfn program. Color shade maps and contour maps of the ELF and LOL for the title molecule are presented in Fig. 8. From the Fig. 8, it can be seen that the covalent regions have high LOL value (red regions), the electron depletion regions between valence shell and inner shell are shown by the blue circles around nuclei. A lone pair of Bromine atom is pointed out by purple arrow while ELF map, the regions around methylene where found to have lesser value where electrons are expected to be delocalized. Whereas the regions around the hydrogen atoms have comparatively large values indicate bonding and nonbonding localized electron. In general, a large ELF or LOL value in a region indicates high localization of electrons (Jacobsen 2009) due to the presence of a covalent bond, a lone pair of electrons, or a nuclear shell in that region. The negative potential is over the

Vol. 6 No. 3 (December, 2021)

electronegative atoms nitrogen and bromine because of the strong intra and intermolecular hydrogen bond. In NCT, on bromine atom have a stronger attraction compared to nitrogen atom. Henceforth these sites intermolecular H-bonding interactions as H-acceptor thus are more sensitive towards the electrophilic attacks. The positive regions of the hydrogen atoms indicate that these sites can be the most possibly involved in nucleophilic processes. These regions of reactivity offer information on the site to be considered for molecular docking of the title molecule with a suitable protein

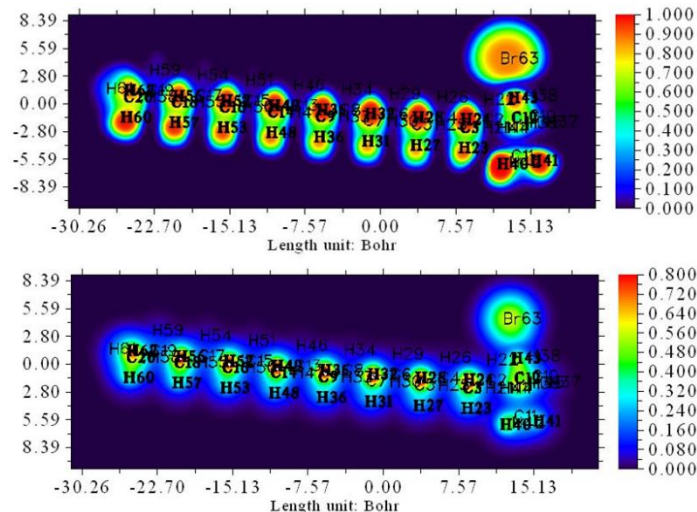


Fig 8 ELF and LOL of NCT

4.6 RDG Analysis

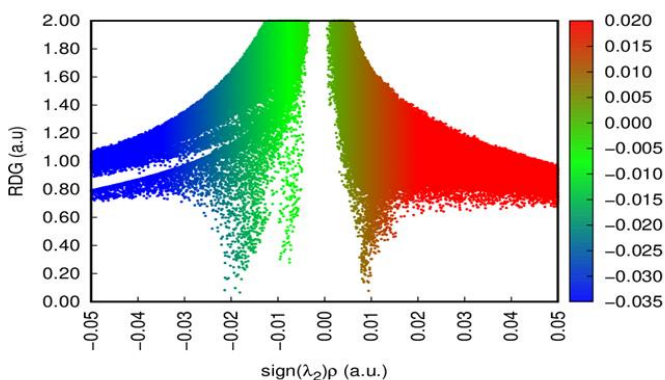


Fig 9 RDG plots of NCT

More recently, reduced density gradient function has been introduced as a tool for revealing non-covalent interactions. Along reactions, interactions change from weak to strong and vice versa and RDG is the basis for reactivity studies [25]. By analysing the low density gradient, low

electron region can be identified and is responsible for weak interaction. Similarly the high density gradient value are used to find the strong interaction. The plot of $r(r)$ against second largest value of Hessian matrix is used to denote the nature and strength of interaction. The interaction of attraction can be defined by $|2 < 0$ and for repulsion $|2 > 0$ [26]. For the title compound, colour and colour/contour filled RDG was drawn using Multiwfn program and are shown in Fig. 9. The blue colour region represents the strong hydrogen bond interactions and the region filled with red colour corresponds to strong repulsion in the ring system and green is surface corresponds to low density region which indicates van der Waals interactions (Margreat, 2010) can be responsible for stabilization of NCT.

4.7 Antimicrobial Analysis

The anti-bacterial activity of the NCT molecule is tested against bacterial strain *Escherichia coli*, *Bacillus cereus*, *Streptococcus pneumoniae*, and *Klebsiella pneumoniae* are shown in Figure 10 and the inhibition diameter are given in Table 3. *E. coli* shows that bacterial species exhibit different sensitivities, and the required results have been compared with the inhibition diameter of positive control with variable extent. The diameter of the inhibition zone of the NCT molecule is 9 mm at 0.1 μ L and 13 mm at 0.2 μ L, and 16 mm at 0.3 μ L the strains *E. coli* and that diameter of inhibition zone revealed anti-bacterial activity. The antibacterial activity of the NCT molecule is tested against some more, because this is higher activity than other strains.

Table 3: Antimicrobial activity of NCT

Bacterial pathogens	Zone of inhibition (mm)		
	0.1 μ L	0.2 μ L	0.3 μ L
<i>Escherichia coli</i>	9	13	16
<i>Bacillus cereus</i>	5	7	12
<i>Streptococcus pneumoniae</i>	7	11	13
<i>Klebsiella pneumoniae</i>	10	13	15

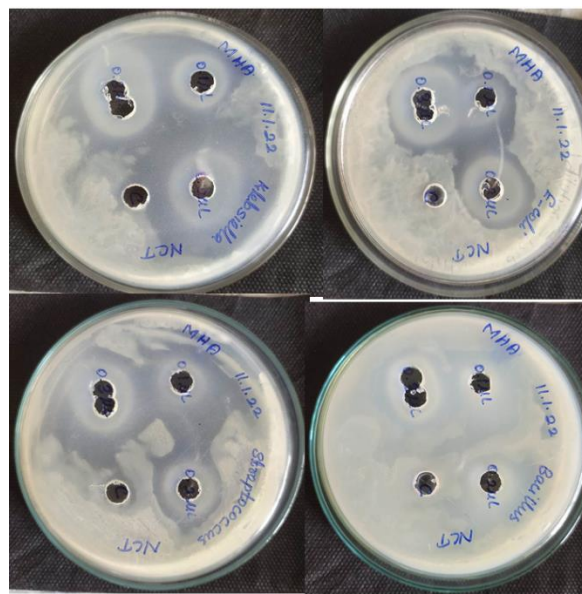


Fig 10 Antimicrobial Activity of NCT

4.8 Drug Likeness

A common and simple approach to measure drug-likeness is property-based rules, which define acceptable boundaries of certain molecular physicochemical properties for drugs and drug candidates. The most famous rule of drug-likeness is "Rule-of-Five" proposed by Lipinski and co-workers, which defines the boundaries of four simple molecular physicochemical properties for orally active compounds [24.] .As there is a wide range of potential medicinal applications for NCT conducted a drug-likeness test on the SwissADME online platform. The molecule including number of hydrogen bond acceptors, donors, value of LogP, Molar refractivity value are summarized in Table 4 and these parameters values that are acceptable for the drug candidate consideration.

Table 4 Drug likeness parameters calculated for title molecule

Descriptors	Calculated	Expected
Molecular mass(Dalton)	363	<500
Hydrogen bond donor	1	<5
Hydrogen bond acceptor	1	<10
Log P	5.8	<5
Molar refractivity	93.47	40-130

5 Conclusions

Charge transfer (CT) reactions of NCT exhibit biological activity. C-H...Br intermolecular hydrogen bonding is important to get a closer insight to these interactions and design those molecules with improved biological profile. Antimicrobial activity results of the viability assay have proved NCT to hold excellent antibacterial activity. Thus, from the above investigations, it can be concluded that NCT is a good antibacterial agent to treat diseases and further work can also be carried out to isolate the exact active moiety responsible for the biological activity.

References

- [1] Laemmli, UK, 1970, 'Cleavage of structural proteins during the assembly of the head of bacteriophage T4', *Nature*, Vol. **227** no.5259, pp.680–685.
- [2] Clarke, Joseph D. (2009-03-01). "Cetyltrimethyl Ammonium Bromide (CTAB) DNA Miniprep for Plant DNA Isolation". *Cold Spring Harbor Protocols*. 2009 (3): pdb.prot5177.
- [3] Azmat, MA, Khan, IA, Cheema, HM, Rajwana, IA, Khan, AS, & Khan, AA, 2012, 'Extraction of DNA suitable for PCR applications from mature leaves of *Mangifera indica* L'. *Journal of Zhejiang University SCIENCE B*, vol. 13, no.4, pp.239–243.
- [4] Emma, I, Kenneth Y, Katz, W, David, K, Sonali BF, H, David, W, Sue, C, Xu, Wei, G, Tabitha WE & Carlo, B, (2009), 'Potential Use of Cetrimonium Bromide as an Apoptosis-Promoting Anticancer Agent for Head and

Neck Cancer', *Molecular Pharmacology*, vol. **76**, no.5, pp. 969–983.

- [5] M.J. Frisch, G.W. Trucks, H.B. Schlegel, G.E. Scuseria, M.A. Robb, J.R. Cheeseman, G. Scalmani, V. Barone, B. Mennucci, G.A. Petersson, H. Nakatsuji, M. Caricato, X. Li, H.P. Hratchian, A.F. Izmaylov, J. Bloino, G. Zheng, J.L. Sonnenberg, M. Hada, M. Ehara, K. Toyota, R. Fukuda, J. Hasegawa, M. Ishida, T. Nakajima, Y. Honda, O. Kitao, H. Nakai, T. Vreven, J.A. Montgomery Jr., J.E. Peralta, F. Ogliaro, M. Bearpark, J.J. Heyd, E. Brothers, K.N. Kudin, V.N. Staroverov, T. Keith, R. Kobayashi, J. Normand, K. Raghavachari, A. Rendell, J.C. Burant, S.S. Iyengar, J. Tomasi, M. Cossi, N. Rega, J.M. Millam, M. Klene, J.E. Knox, J.B. Cross, V. Bakken, C. Adamo, J. Jaramillo, R. Gomperts, R.E. Stratmann, O. Yazyev, A.J. Austin, R. Cammi, C. Pomelli, J.W. Ochterski, R.L. Martin, K. Morokuma, V.G. Zakrzewski, G.A. Voth, P. Salvador, J.J. Dannenberg, S. Dapprich, A.D. Daniels, O. Farkas, J.B. Foresman, J.V. Ortiz, J. Cioslowski, D.J. Fox, Gaussian 09, Revision C.02, Gaussian Inc., Wallingford CT, 2010
- [6] E. Runge, E.K.U. Gross, *Phys. Rev. Lett.* 52 (1984) 997–1000.
- [7] M. Petersilka, U.J. Gossmann, E.K.U. Gross, *Phys. Rev. Lett.* 76 (1966) 1212–1215.
- [8] R. Bauernschmitt, R. Ahlrichs, *Chem. Phys. Lett.* 256 (1996) 454–464.
- [9] C. Jamorski, M.E. Casida, D.R. Salahub, *J. Chem. Phys.* 104 (1996) 5134–5147
- [10] E.D. Glendening, A.E. Reed, J.E. Carpenter, F. Weinhold, NBO Version 3.1, TCI, University of Wisconsin, Madison, 1998.
- [11] T. Lu, F. Chen, Multiwfn: a multifunctional wave function analyser, *J. Comput. Chem.* 33 (2012) 580–592.
- [12] B. Fathima Rizwana, J. Christian Prasanaa, S. Muthu, Christina Susan Abraham, *Comp. Biology and Chemistry* 78 (2019) 9–17,
- [13] W. Humphrey, A. Dalke, K. Schulten, VMD: visual molecular dynamics. *J. Mol. Graph.* 14(1996) 33–38.
- [14] Rovira, MC, Novoa, JJ, Whangbo, MH & Williams, JM, 1995, 'Ab initio computation of the potential energy surfaces of the water-hydrocarbon complexes H₂O-C₂H₂, H₂O-C₂H₄ and H₂O-CH₄: minimum energy structures, vibrational frequencies and hydrogen bond energies', *The Journal of Chemical Physics*, vol. 200, pp. 319–335.
- [15] Varsanyi, G, 1974, 'Assignments for Vibrational Spectra of Seven Hundred Benzene Derivatives', vol. I, Adam Hilger, London.
- [16] Colthup, NB, Daly LH & Wiberly, SE 1990, 'Introduction to Infrared and Raman Spectroscopy', Academic Press, New York.
- [17] Smith, BC 1996, *Infrared Spectral Interpretation – A Schematic Approach*, CRC Press, New York.
- [18] Beaula, JT, Muthuraja, P, Dhandapani, M & Jothy, VB, 2018, 'Effect of charge transfer with spectral analysis on

- the antibacterial compound 4-(Dimethyl amino) pyridine: 3,5-Dinitrobenzoic acid: Experimental and theoretical perspective', *Journal of Molecular Structure*, vol. 1171, pp.511-526
- [19] Poizat, O &Guichard, VJ 1989, 'Vibrational studies of reactive intermediates of aromaticamines. IV. Radical cation time-resolved resonance Raman investigation of N, N-dimethylaniline and N, N-diethylaniline derivatives', *Journal of Chemical Physics*, vol.90, pp.4697-4703.
- [20] Okamoto, H, Inishi, H, Nakamura, Y, Kohtani, S &Nakagaki, R 2000, 'Infrared and Raman spectra of 4-(dimethyl amino)benzonitrile and isotopomers in the ground state and vibrational analysis', *Chemical Physics*, vol.260, no.1-2, pp.193-214.
- [21] Hiremath, SM, Suvitha, A, Patil, NR, Hiremath, CS, Khemalpure, SS, Pattanayak, SK, Negalurmath, VS &Obelannavar, K, 2018, 'Molecular structure, vibrational spectra, NMR, UV, NBO, NLO, HOMO-LUMO and molecular dockingof2-(4, 6-Dimethyl-1-benzofuran-3-yl) acetic acid (2DBAA): experimental andtheoretical approach', *Journal of Molecular Structure*, vol. 1171, pp. 362-374.
- [22] Hiremath, SM, Suvitha, A, Patil, NR, Hiremath, CS, Khemalpure, SS, Pattanayak, SK, Negalurmath, VS, Obelannavar, K, Armakovic& SJ, Armakovic, S, 2018, 'Synthesis of 5-(5-methyl-benzofuran-3-ylmethyl)-3H-[1, 3, 4]oxadiazole-2-thione and investigation of its spectroscopic, reactivity, optoelectronicand drug likeness properties by combined computational and experimental approach', *SpectrochimicaActa Part A: Molecular and Biomolecular Spectroscopy*, vol.205, pp.95-110.
- [23] Okamoto, H, Inishi, H, Nakamura, Y, Kohtani, S &Nakagaki, R 2000, 'Infrared and Raman spectra of 4-(dimethyl amino)benzonitrile and isotopomers in the ground state and vibrational analysis', *Chemical Physics*, vol.260, no.1-2, pp.193-214.
- [24] Lipinski, CA 2004, 'Lead- and drug-like compounds: the rule-of-five revolution', *Drug Discovery Today: Technologies*, vol.1, no.4, pp.337-341
- [25] Boto, RA &Piquemal, JP, 2017, 'Contreras-Garcia, Revealing strong interactions withthe reduced density gradient: a benchmark for covalent, ionic and charge shift bonds', *Journal Theoretical Chemistry Accounts*, pp. 136-139.
- [26] Johnson, ER, Keinan, S, Mori-Sánchez, P, Contreras-García, J, Cohen, AJ & Yang, W 2010, 'Revealing Noncovalent Interactions', *Journal of American Chemical Society*, vol.132, pp. 6498-6506.